Experimental and Numerical Investigation of Nozzle Jet Velocity Effects on Parallel Jet Combustor Characteristics of Hydrogen Enriched Fuel

LIU Zhi-gang[1,2], XIONG Yan[1,2], ZHANG Zhe-dian[1,2]

(1. Key Laboratory of Advanced Energy and Power, Institute of Engineering Thermophysics, Chinese Academy of Sciences, Beijing 100190, China;
2. University of Chinese Academy of Sciences, Beijing 100049, China)

Abstract: Adding hydrogen into natural gas fuelled for gas turbines is a feasible strategy for reducing carbon emissions. Moderate or Intense Low Oxygen Dilution (MILD) combustion has potential to solve the problem of high NO_x emissions for high adiabatic flame temperature. The effects of jet velocity on the characteristics of parallel jet combustor were studied through experimental investigations and numerical simulations. The fuel is consisted of 50% methane and 50% hydrogen by volume. The jet velocity ranged from 90m/s to 150m/s. Based on a simplified chemical reactor network model, the threshold recirculation ratio for MILD combustion of hydrogen enriched fuel under different adiabatic flame temperatures was calculated according to the experimental conditions. When the equivalent ratio is less than 0.6, the threshold recirculation ratio decreases with the increase in the hydrogen fraction. The experimental results show that NO_x emissions decrease slightly, and CO emissions and the lift-off height of reaction zone increase as the jet velocity increases. When the nozzle jet velocity changes from 90m/s to 150m/s, the numerical simulation results show that the proportion of flue gas recirculation in the parallel jet combustor remains unchanged. However, the region with $Da>1$ decreases to visualise the effect of jet velocity of MILD combustion of hydrogen enriched fuel, which means that the region of slow-chemistry reaction increases. For hydrogen enriched fuel, increasing the jet velocity is conducive to establishing MILD combustion and meeting the requirement of low NO_x emissions.

Key words: MILD combustion; Hydrogen enriched fuel; NO_x emissions; Lift-off height; Damköhler number

CLC number: V231.1　**Document code**: A　**Article number**: 1001-4055 (2023) 11-210840-10

DOI: 10.13675/j.cnki. tjjs. 210840

喷嘴射流速度对富氢燃料平行射流燃烧器燃烧特性影响的实验和数值研究 *

刘志刚[1,2]，熊　燕[1,2]，张哲巅[1,2]

（1. 中国科学院工程热物理研究所 先进能源动力重点实验室，北京 100190；
2. 中国科学院大学，北京 100049）

摘　要：针对燃气轮机燃烧，天然气掺氢是减少碳排放的可行策略。柔和燃烧（Moderate or Intense

* **收稿日期**：2021-12-02；**修订日期**：2022-03-02。
基金项目：National Science and Technology Major Project of China (2019-Ⅲ-0018-0062)。
作者简介：刘志刚，博士生，研究领域为低污染燃烧技术。
通讯作者：熊　燕，博士，高级工程师，研究领域为低污染燃烧技术及燃烧室设计。
引用格式：刘志刚，熊　燕，张哲巅. 喷嘴射流速度对富氢燃料平行射流燃烧器燃烧特性影响的实验和数值研究[J]. 推进技术，2023，44（11）：210840. （LIU Zhi-gang, XIONG Yan, ZHANG Zhe-dian. Experimental and Numerical Investigation of Nozzle Jet Velocity Effects on Parallel Jet Combustor Characteristics of Hydrogen Enriched Fuel [J]. *Journal of Propulsion Technology*, 2023, 44(11): 210840.）

Low Oxygen Dilution）具备解决高绝热火焰温度下NOx排放过高的潜力。本文通过实验和数值模拟相结合的方式，研究了喷嘴射流速度对富氢燃料平行射流燃烧器燃烧特性的影响。实验燃料由Vol.50%甲烷和Vol.50%氢气构成。喷嘴的射流速度为90~150m/s。基于实验工况，利用化学反应网络模型计算了富氢燃料在不同绝热火焰温度下实现柔和燃烧的临界回流比。当量比小于0.6时，临界回流比随着氢气含量的增加而降低。实验结果表明，喷嘴射流速度的增加，NOx排放略有下降，CO排放和反应区抬升高度增加。喷嘴喷射速度由90m/s增加到150m/s，数值模拟结果显示，平行喷射燃烧器内的烟气回流比例保持不变。Da数（Damköhler number）的分布可作为判定柔和燃烧的因素，其直观显示喷嘴射流速度对柔和燃烧的影响。喷嘴射流速度增加，流场内Da>1的区域呈现降低趋势，这意味着慢速反应区域增加。对于富氢燃料，提高喷嘴射流速度有利于建立柔和燃烧，达到低NOx排放。

关键词：柔和燃烧；富氢燃料；NOx排放；抬升高度；Da数

Nomenclature

T_{in-air}/K	Inlet air temperature	Z/D	Axial position
$T_{in-fuel}$/K	Inlet fuel temperature	τ_{mix}/s	Residence time
T_{si}/K	Self-ignition temperature	τ_{chem}/s	Reaction time
T_{mix}/K	Temperature of the mixture	C_p/(J/(kg·K))	Specific heat capacity
ΔT/K	Reaction temperature rise	S_L/(m/s)	Laminar flame speed
T_{out}/K	Outlet temperature	d/m	Characteristic length
T_b/K	Measured temperature	d_b/m	Characteristic length of the thermocouple
m_g/(kg/s)	Mass of recalculating flue gas	d_{nozzle}/m	Diameter of nozzle
m_a/(kg/s)	Mass of inlet air	$\bar{v}$/(m/s)	Velocity of mixture
m_f/(kg/s)	Mass of inlet fuel	λ/(W/(m·K))	Thermal conductivity
ρ/(kg/m^3)	Density	δ_L/m	Laminar flame thickness
ρ_g/(kg/m^3)	Density of flue gas	α/(m^2/s)	Thermal diffusion coefficient
v_z/(m/s)	Normal velocity at the element of cross section	$Q_{V,air}$/(m^3/h)	Air bulk flow under standard condition
dA/m^2	Area of the cross-sectional element	Q_V/(m^3/h)	Bulk flow rate
A_{nozzle}/m^2	Exit cross-sectional area of four nozzles	v_j/(m/s)	Jet velocity of nozzle
D/m	Diameter of combustion chamber	v_g/(m/s)	Velocity of flue gas
r/m	Radius of combustion chamber	Φ_{global}	Global equivalence ratio
R	Recirculation ratio	μ_g/(Pa·s)	Dynamic viscosity of flue gas
$R_{threshold}$	Threshold recirculation ratio	ε	Emissivity of thermocouple

1 Introduction

As a clean energy source, hydrogen can effectively reduce CO_2 emissions and contribute to achieving the national goal of carbon emissions peak and carbon neutrality [1-2]. Considering the imperfect distribution facilities of hydrogen infrastructure, hydrogen blending natural gas is a feasible way to transfer to hydrogen energy [3]. Meanwhile, existing natural gas pipeline is used to transport hydrogen blending natural gas (20 Vol.% H_2) without any modification of the pipeline. In order to further reduce carbon emissions, it is necessary to investigate the combustion characteristics of hydrogen blending natural gas with higher hydrogen fraction. However, the addition of hydrogen increases the temperature of local reaction zone and flame propagation speed [4]. The novel combustion technology is needed to solve the problem of NOx emission increase and flashback caused by hydrogen addition.

It has been proved that the Moderate or Intense Low Oxygen Dilution (MILD) combustion has the characteristics of low pollutant emission and stable combustion for hydrogen enriched fuel [5-7]. Lingstädt et al. [8] proposed the concept of solid oxide fuel cell and micro gas turbine (SOFC/MGT) for low calorific value fuel with 5%~10% hydrogen fraction, and improved the overall efficiency of gas turbine. Low calorific value fuel with hydrogen fraction up to 30% by volume has been tested on Flameless Oxidation (FLOX) combustor by jetting induced flue gas recirculation, and NOx emissions remain consistent below 1×10^{-5}@15%O_2 [9]. For axial staged combustor, experimental results show that uniformity of the secondary reaction zone is realized by increasing velocity of secondary nozzle for hydrogen enriched fuel [10]. Using the method of numerical simulation, Mardani et al[11]. studied the influence of jet velocity on Jet-in-Hot-Coflow (JHC) combustor. The results show that increasing the jet velocity is beneficial to the expanding combustion zone. For hydrogen enriched fuel with 40 Vol.% hydrogen, NOx emissions of FLOX combustor show a decreasing trend when jet velocity of nozzle increases from 90m/s to 160m/s [12]. For the MILD combustor, the specific reason why increasing the jet velocity can reduce NOx emissions is not explained in detail, whether it increases the proportion of flue gas recirculation or increases the ignition delay time of unburned reactants for higher hydrogen concentration.

In this paper, the effects of nozzle jet velocity on pollutant emissions and the distribution of reaction zone of hydrogen enriched fuel in a parallel jet combustor were investigated. Combined with a simplified Chemical Reactor Network (CRN) model, the influences of hydrogen fraction of hydrogen enriched fuel on the formation conditions of MILD combustion were carried out. In addition, the flue gas recirculation ratio along the axial direction, CH_2O distribution and Da distribution of the combustor were analyzed by CFD simulations to supplement the explanation for jet velocity effects on the combustion of hydrogen enriched fuel.

2 Methodology

2.1 Experimental configurations

The experimental system diagram of the parallel jet combustor system is shown in Fig. 1. The combustion system is mainly composed of a parallel jet combustor, a fuel mixer, fuel supply system, air supply system, flue gas measurement system and reaction zones measurement system. Hydrogen and methane are stored separately in high-pressure holders, which are regulated efficiently and accurately by mass flow meters. The mixing of hydrogen and methane is accomplished in the cylindrical fuel mixer, which finally enters the parallel jet

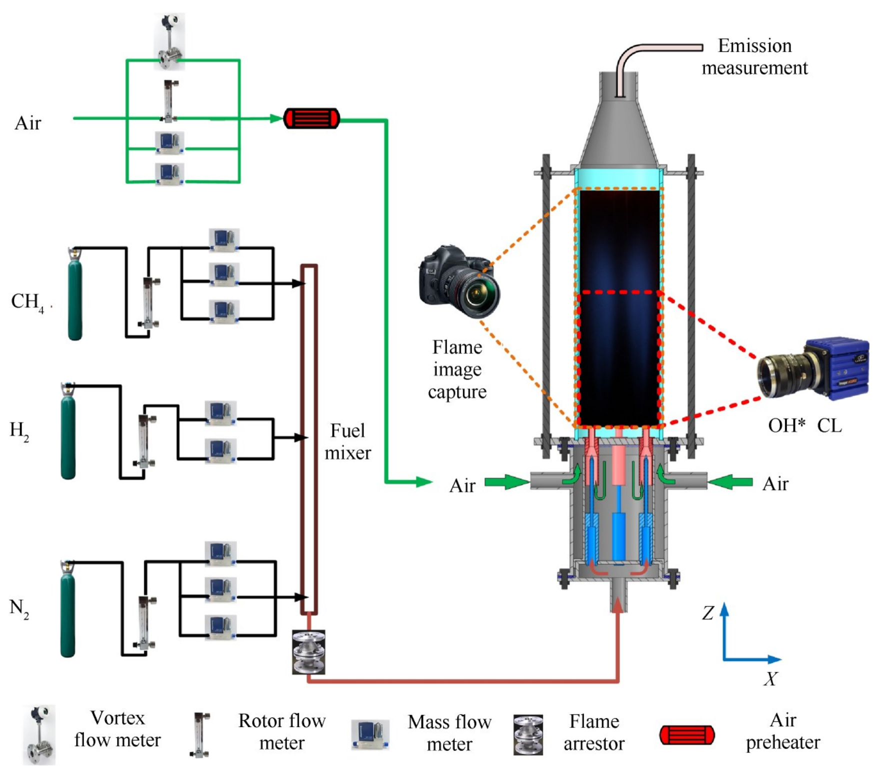

Fig. 1 Sketch of the parallel jet combustor system

burner. Four axial jet nozzles with 8mm diameter of the parallel jet combustor create a large reflux zone inside the combustor achieving the mixing of high temperature flue gas and unburned reactants. The mixing temperature was greater than the self-ignition temperature, which was the flame-stabilizing mechanism of parallel jet burner. The specific structure of the combustor has been described in detail in previous studies[13]. The composition of flue gas is measured using a flue gas analyzer. Canon camera and ICCD camera are combined to capture the distribution of reaction zone.

2.2 Optical OH* measurements

The OH* Chemiluminescence system (OH* CL) provided by LaVision was used to measure and analyze the structure of combustion reaction zone in the parallel jet combustor. The OH* signal was extensively used to qualitatively characterize the location and structure of the heat release zone for MILD combustion [9, 14]. The ICCD camera was equipped with a narrow-band filter to capture the OH* distribution. The parameter of the filter was BP308±10nm, and the resolution of the ICCD camera was 1600×1200pixels. 200 frames of OH* transient images were captured continuously at each steady state and homogenized to obtain the structure and location of the reaction zone. In order to obtain the location and lift-off height of reaction zone more intuitively, the OH* images were processed by extracting contours to obtain the boundary of reaction zone [15]. Firstly, the color scale was unified and the maximum OH* signal intensity ($\mathrm{Max}(\mathrm{OH}_n^*)$) was extracted for all experimental conditions, and the maximum extracted values ($\mathrm{Max}(\mathrm{Max}(\mathrm{OH}_1^*), \cdots, \mathrm{Max}(\mathrm{OH}_n^*))$) was used as the upper limit of color scale. Secondly, the maximum extracted value of 10% was used as a criterion for boundary extraction.

2.3 Emissions measurements

The flue gas compositions were measured in the experiments by Testo 350 flue gas analyzer, including O_2, CO, NO, NO_2 and UHC (Unburned hydrocarbon). The accuracy of O_2 measurement was ±0.2 Vol.%, and the accuracy of NO, NO_2 and CO measurement was ± 5% of measured value. To ensure the accuracy of flue gas measured, each experimental condition was measured continuously for 30s after stabilization. In order to better compare the emission results under different experimental conditions, NOx and CO fractions were corrected by converting to 15% oxygen concentration, abbreviated as $\times 10^{-6}$@15%O_2.

2.4 Experimental conditions

Taking into account the combustion heat load and nozzle pressure loss, the experimental nozzle jet velocity ranged from 90m/s to 150m/s, adjusted by changing the air volume flow rate. As shown in Eq. (1), when the nozzle diameter was certain, volume flow rate and jet velocity of the nozzle were linearly related. The air volume flow rates under standard condition were 60m^3/h, 80m^3/h and 100m^3/h, respectively. The pressure of standard condition was 101325Pa, and the temperature of standard condition was 0℃.

$$\begin{aligned} Q_\mathrm{V} &= v_\mathrm{j} \cdot A_\mathrm{nozzle} \\ &= v_\mathrm{j} \cdot 4 \cdot \frac{1}{4} \pi d_\mathrm{nozzle} \\ &= \pi \cdot v_\mathrm{j} \cdot d_\mathrm{nozzle} \end{aligned} \tag{1}$$

where Q_V is bulk flow rate, v_j is the jet velocity of nozzle, A_nozzle is the exit cross-sectional area of four nozzles and d_nozzle is the diameter of nozzle.

Pure methane was used to replace natural gas in the experiment. The purity of methane was 99.9%. The purity of hydrogen was 99.99%. Hydrogen enriched fuel consisted of 50 Vol.% hydrogen and 50 Vol.% methane. The combustor outlet pressure was ambient pressure. $Q_\mathrm{V,air}$ was the air bulk flow under standard condition. The specific experimental conditions were shown in Table 1.

2.5 CRN model setup

Combined with GRI 3.0 mechanism, a simplified CRN model [10, 16] was established to theoretically analyze the influence of hydrogen fraction on MILD combus-

Table 1　Experimental conditions

$Q_\mathrm{V,air}$/(m^3/h)	$T_\mathrm{in-air}$/K	Fuels	$T_\mathrm{in-fuel}$/K	v_j/(m/s)	Re	Φ_global
60	289	50 Vol.% H_2	289	90	49145	0.49 ~ 0.59
80	289	50 Vol.% H_2	289	120	65527	0.49 ~ 0.55
100	289	50 Vol.% H_2	289	150	81908	0.49 ~ 0.54

tion. As shown in Fig. 2, a Perfectly Stirred Reactor (PSR) was used to simulate the generation of flue gas, a mixer was used to simulate the mixing of flue gas and fresh reactants, and a Closed Homogeneous Batch Reactor (CHBR) was used to calculate the self-ignition temperature (T_{si}) of the mixture. Referred to the PSR-like definition [17], the temperature of the mixture (T_{mix}) was higher than the self-ignition temperature, and the reaction temperature rise ($\Delta T = T_{out} - T_{mix}$) was lower than the self-ignition temperature when MILD combustion occurred.

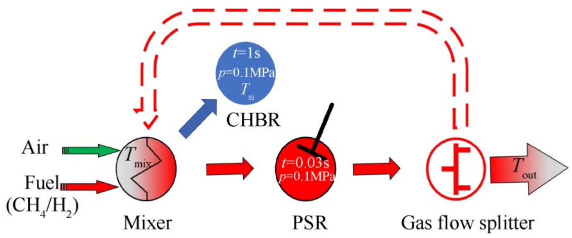

Fig. 2 Simplified CRN model for MILD combustion

2.6 CFD model setup

The Reynolds-Averaged Navier-Stokes (RANS) approach was adopted along the Eddy Dissipation Concept (EDC) combustion model with DRM19 mechanism[18], including 19 species (plus Ar and N_2) and 84 reversible reactions. The numerical method was SIMPLE. The radiation model was the Discrete Ordinate (DO) technique, combined with the Weighted Sum of Gray Gases (WSGG) absorption emission model. The boundary conditions of air and fuel were set to mass flow inlet with a turbulence intensity of 0.05. The boundary conditions of outlet were set to the pressure outlet. The wall conditions were set to adiabatic and no-slip. The validation of the numerical simulation method has been demonstrated in our previous work [13, 16] and the FLOX combustor [19]. In order to select a suitable turbulence model for the parallel jet combustor, results of different turbulence models were compared with the experimental results. For Jet-in-Hot-Coflow combustor (JHC), the modified $k-\varepsilon$ model ($C_{1\varepsilon}$ adjusted from 1.44 to 1.60) is found to better reproduce experimental data [20]. Lewandowski et al[21]. proved that the standard $k-\varepsilon$ model appeared to give the most satisfactory results for Delft Jet-in-Hot-Coflow (DJHC) combustor. The realizable $k-\varepsilon$ turbulence model agree well with the experiment at different heights for the furnace with optical accesses and upstream recirculation (FOUR) [16]. For the parallel jet combustor, the turbulence models to be verified were standard $k-\varepsilon$ model (SKE), realizable $k-\varepsilon$ model (RKE), RNG $k-\varepsilon$ model and modified $k-\varepsilon$ model. Fig. 3 shows comparison of numerical simulation and experimental results under cold conditions according to the cold flow field data with air volume flow rate of $100m^3/h$ and nozzle diameter of 10mm. As shown in Fig.3, the results showed that the simulation results of standard $k-\varepsilon$ were closer to the experimental results at different axial positions, and the simulation results well predicted the performance of parallel jet combustor. The x/r was the radial relative position, where r was the radius of combustion chamber.

By adjusting the grid size of the locally densified areas and the global grid size, three grids with different densities were generated for grid independent verification. According to the characteristics of the burner, the areas with a great influence on the flow field were locally densified, which were divided into three zones (boi 1, boi 2 and boi 3. boi (body of influence)). The number of grid cells was 0.88 million, 1.3 million and 2.2 million, respectively. For the experimental condition of air volume flow rate of $100m^3/h$, the axial velocities on the central axis of combustion chamber and nozzle were compared and analyzed. As shown in Fig. 4, the axial velocity was basically the same for the results of grids 1.3 million and 2.2 million. Considering the cost and time of calculation, the grid with the number of 1.3 million was finally chosen for the numerical calculation.

3 Results and discussion

3.1 Threshold recirculation ratio

The effects of hydrogen fraction on threshold recirculation ratio generated by MILD combustion were analyzed using CRN model. As shown in Fig.5, compared to methane fuels, the threshold recirculation ratio ($R_{threshold}$) tended to decrease with an increase in the hydrogen fraction when the equivalence ratio was less than 0.6, which facilitated the occurrence of MILD combustion. However, when the equivalent ratio was greater than 0.65, the threshold recirculation ratio increased. Compared with methane, MILD combustion of hydrogen

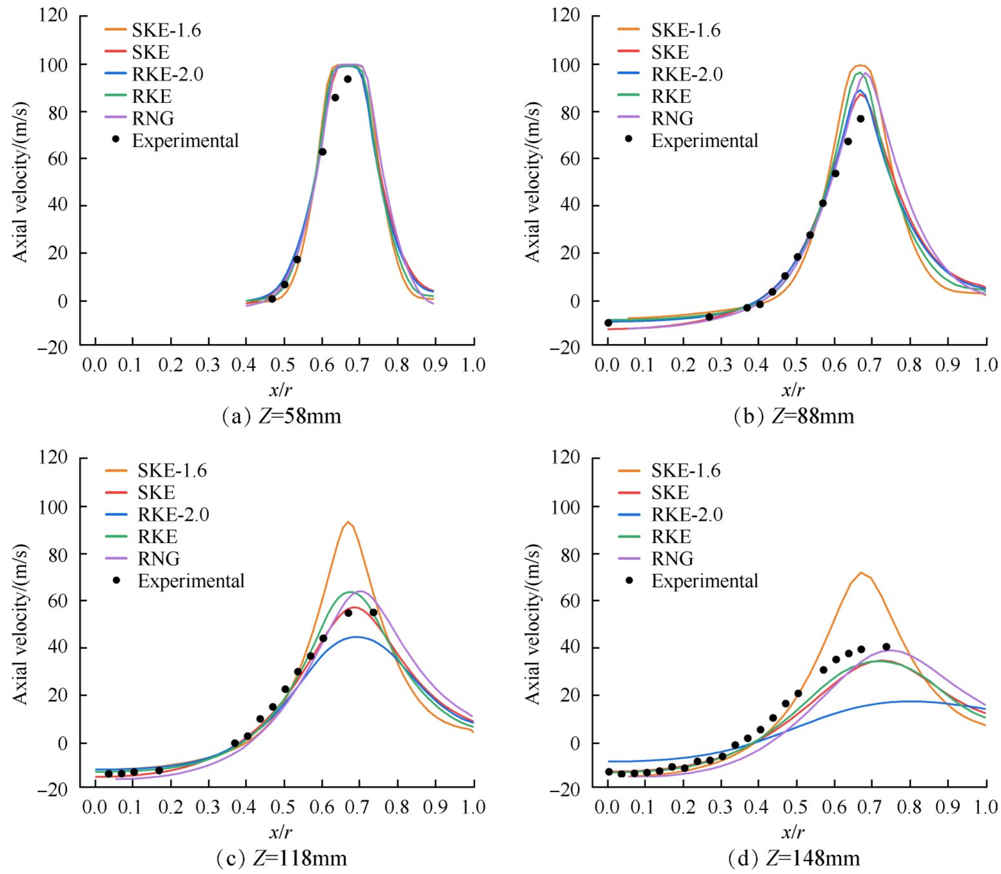

Fig. 3　Turbulence model validation

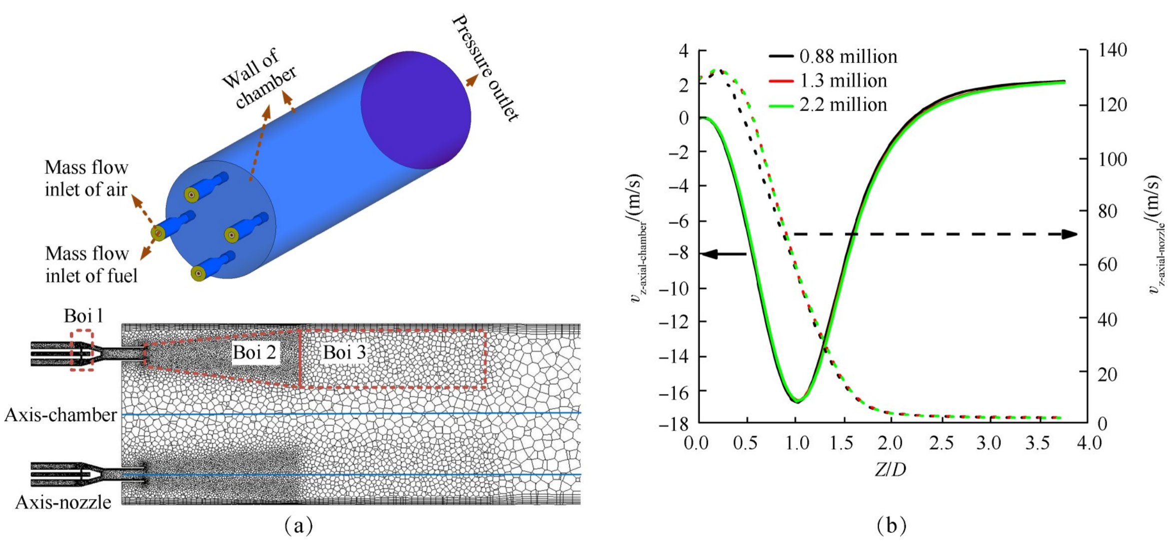

Fig. 4　Mesh independence verification

enriched fuel was easier to organize at low equivalence ratios, regardless of ignition delay time.

To quantitatively describe the effect of jet velocity on flue gas recirculation, the flue gas return ratio is defined as Eq.(2).

$$R = \frac{m_g}{m_a + m_f} = \frac{\iint_A \rho\left(\left|v_z\right| - v_z\right)\mathrm{d}A}{2(m_a + m_f)} \tag{2}$$

Where m_g, m_a and m_f are mass of recirculating flue gas, mass of inlet air, and mass of inlet fuel, respectively. ρ is the density of the mixture at the element of cross section. v_z is the normal velocity at the element of the cross section. dA is the area of the cross-sectional element.

As shown in Fig. 6, the flue gas recirculation ratio (R) of cold flow field along axial direction was extracted

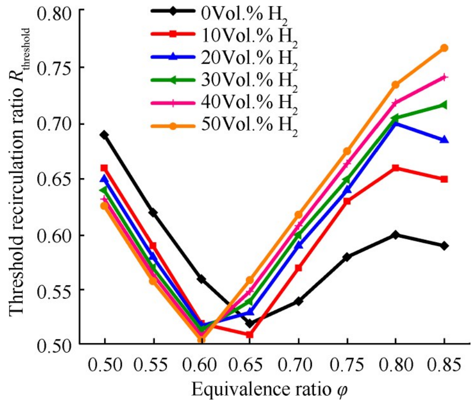

Fig. 5　Effect of hydrogen fraction on threshold recirculation ratio

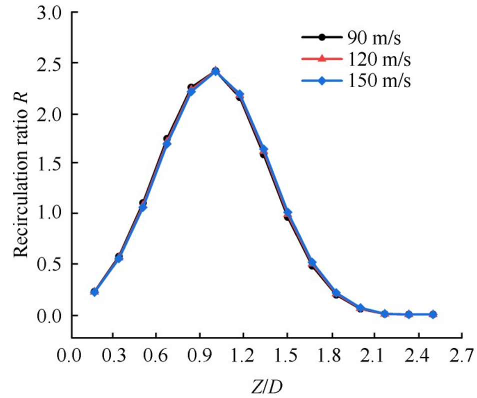

Fig. 6　Influence of jet velocity on recirculation ratio

by numerical simulation. At the axial position of Z/D=1, the flue gas recirculation ratio was the largest. The D was the diameter of combustion chamber. Considering that the experimental condition equivalent ratio is less than 0.6, the threshold recirculation ratio of MILD combustion was satisfied in the region of axial position Z/D= 0.5 to 1.5 within the parallel jet combustor. When the nozzle jet velocity reached 90m/s, further increasing the nozzle velocity unchanged the ratio of reflux in the combustor.

3.2　NO*x* and CO emissions

The influence of nozzle jet velocity on combustion characteristics of parallel jet combustor is shown in the Fig.7 obtained by experiment. The combustor outlet temperature was measured with an exposed type B thermocouple. According to Newton's law of cooling and heat radiation law, the radiation error of flue gas temperature was corrected. The corrected flue gas temperature is defined as Eq.(3).

$$T_{out} = T_b + \frac{1.25\varepsilon\sigma T_b^4 d_b^{0.75}}{\lambda}\left(\frac{\mu_g}{\rho_g v_g}\right)^{0.25} \tag{3}$$

Where T_{out} and T_b are the outlet temperature and measured temperature, respectively. ε is the emissivity of thermocouple. σ is the radiation constant of black body. ρ_g is the density of flue gas. d_b is the characteristic length of the thermocouple. μ_g is the dynamic viscosity of flue gas. v_g is the velocity of flue gas. λ is the thermal conductivity. The thermal conductivity and dynamic viscosity of the flue gas at different temperatures were calculated by the GASEQ software.

At the same outlet temperature of combustion chamber, NO*x* emissions slightly decreased and CO emissions increased as the jet velocity increased. With the increase of jet velocity, the residence time of flue gas was shortened which was not conducive to the burnout of CO.

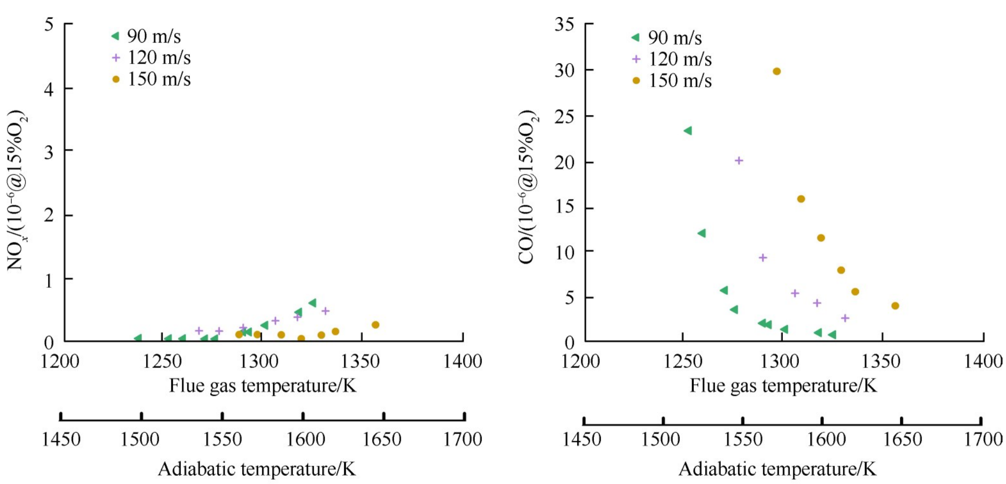

(a) NO_x emissions　　(b) CO emissions

Fig. 7　Effect of jet velocity on pollutant emission obtained by experiment

3.3 Reaction zone distribution

Shown in Fig. 8 are the captured flame image and OH* CL for the 50 Vol.% H_2 hydrogen enriched fuel at different jet velocities and equivalent ratios. From the flame image, the flame zone was extended with increasing jet velocity at the same equivalent ratio. The same flue gas oxygen concentration was guaranteed at the three conditions, fluctuated within 0.2 Vol.% which was the accuracy of O_2 measurement, determining the same equivalence ratio. When the equivalent ratio was 0.5, the combustion reaction zone was uniformly distributed at different jet velocities, which was close to the state of distributed combustion. From the OH* CL diagram, when the nozzle velocity increased, lift-off height of the reaction zone increased. Increasing the jet velocity of the nozzle is conducive to achieving MILD combustion.

According to the experimental condition of equivalence ratio of 0.53, numerical simulations were conducted to further analyze the influence of jet velocity on the temperature distribution, CH_2O distribution and Da number in the combustion zone, as shown in Fig. 9.

As the jet velocity increased, temperature at the head and exit of the combustor decreased, and the temperature uniformity across reaction zone improved. As a key combustion intermediate, the normalized CH_2O ($CH_2O_{\text{mole fraction}}/CH_2O_{\text{mole fraction, max}}$) is used to characterize the distribution of flame preheating zone [22]. The distribution of normalized CH_2O expanded along the axial and radial direction with the increase of jet velocity. The Da distribution showed that the region with $Da > 1$ shrunk as the jet velocity increased, which in turn verified that the jet velocity was conducive to the organization of MILD combustion of hydrogen enriched fuel. Da number was used as Eq. (4).

$$Da = \frac{\tau_{\text{mix}}}{\tau_{\text{chem}}} = \frac{\rho C_{\text{P}} S_{\text{L}}{}^{2} d}{\lambda \bar{v}} \tag{4}$$

$$\tau_{\text{mix}} = \frac{d}{\bar{v}} \tag{5}$$

$$\tau_{\text{chem}} = \frac{\delta_{\text{L}}}{S_{\text{L}}} = \frac{\alpha}{S_{\text{L}}{}^{2}} \tag{6}$$

$$\alpha = \frac{\lambda}{\rho C_{\text{P}}} \tag{7}$$

Where τ_{mix} and τ_{chem} are the residence time and reaction

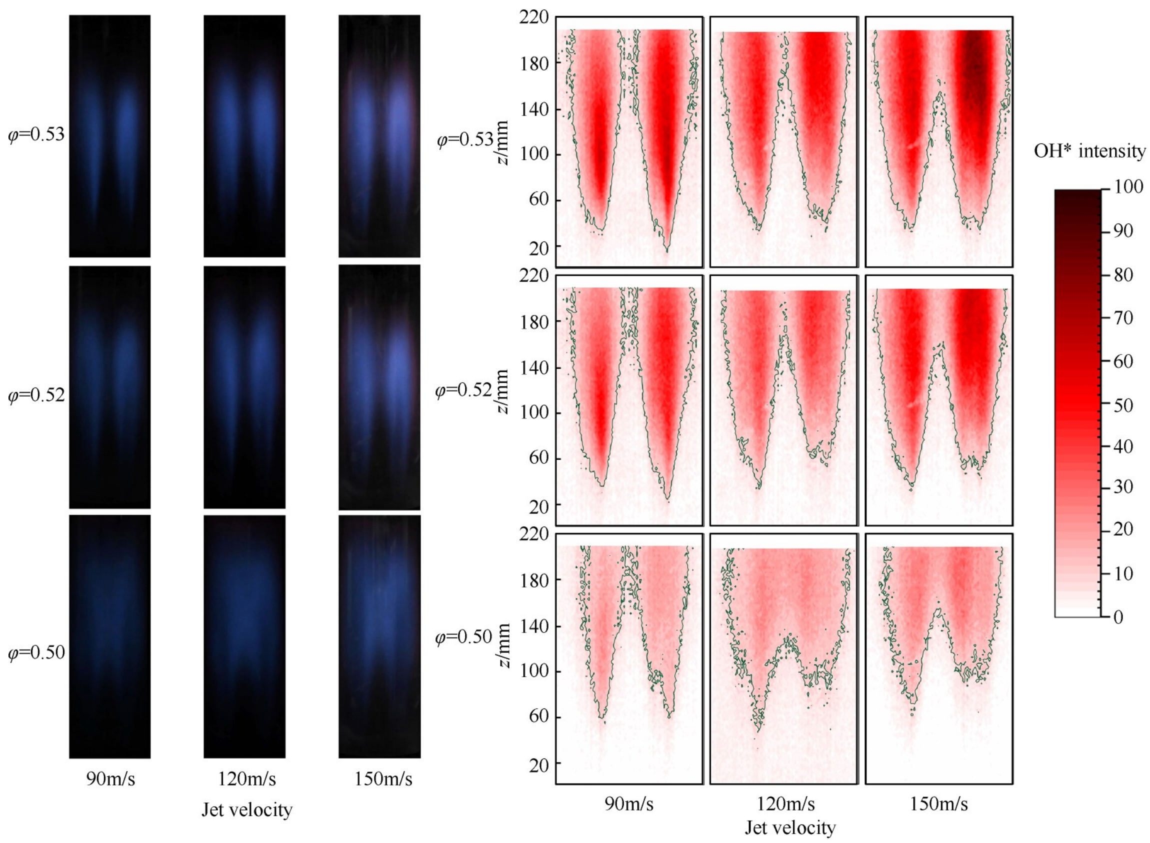

(a) Flame image　　(b) OH* image

Fig. 8　Effect of jet velocity on reaction zone

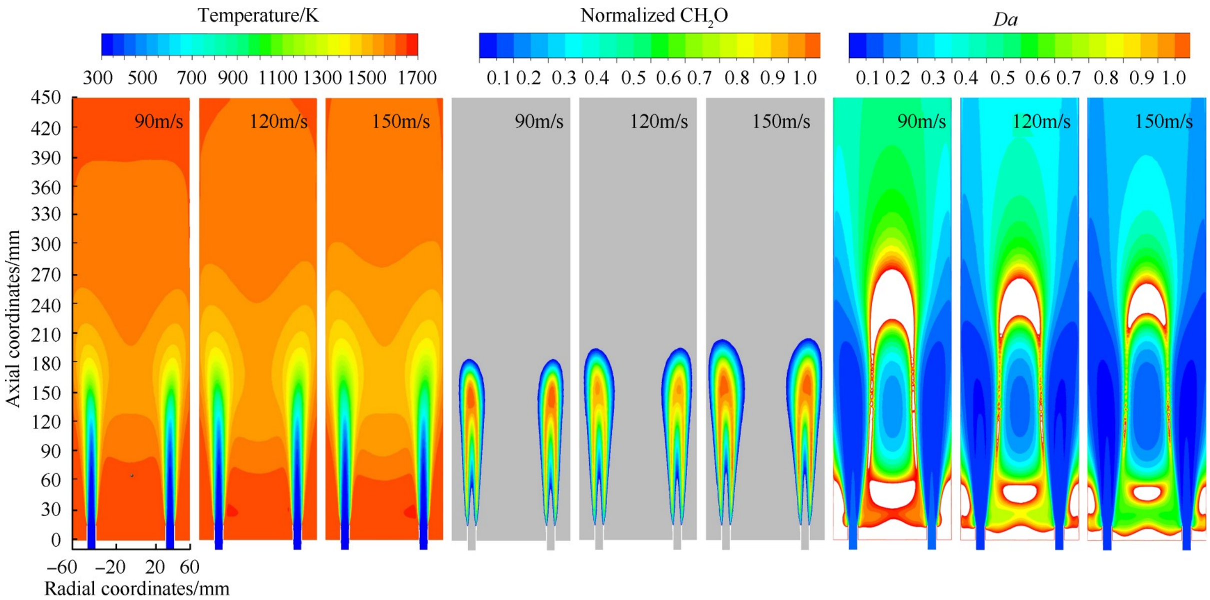

(a) Temperature　(b) Normalized CH_2O　(c) *Da*

Fig. 9　Effect of jet velocity on reaction zone distribution

time of mixture respectively. C_P is the specific heat capacity of mixture. S_L is the laminar flame speed of reactants. ρ is the density of the mixture. d is the characteristic length of the combustor. $\bar{v}$ is the velocity of the mixture. λ is the thermal conductivity. δ_L is the laminar flame thickness of reactants. α is the thermal diffusion coefficient of mixture.

4　Conclusions

A simplified CRN model was established to analyze the influence of hydrogen fraction of hydrogen-rich fuel on the threshold recirculation ratio of MILD combustion. At the equivalence ratio less than 0.6, the threshold recirculation ratio to achieve MILD combustion tended to decrease with increasing hydrogen fraction at atmospheric pressure and temperature conditions, which was favorable to the occurrence of MILD combustion. However, this was not the case when the equivalence ratio was greater than 0.65.

At equivalence ratios below 0.6, the effects of nozzle jet velocity on the combustion characteristics of hydrogen-rich fuel with 50 Vol.% H_2 were investigated on the parallel jet combustor. NOx emissions slightly decreased with increasing jet velocity, while CO emissions and lift-off height of the reaction zone increased when the jet velocity increased at the same equivalence ratio.

Combined with the CFD simulation results, a variation of the flue gas internal recirculation ratio and *Da* distribution with jet velocity were analyzed. The results of numerical simulations show that when the jet velocity changes from 90m/s to 150m/s, the flow pattern inside the parallel jet combustor remains similar. Increasing the jet velocity extended the preheat zone in the axial and radial directions, and the region with $Da>1$ shrunk, which is conducive to the establishment of MILD combustion.

Acknowledgement: The authors gratefully acknowledge the support provided by National Science and Technology Major Project of China.

References

[1] Voldsund M, Jordal K, Anantharaman R. Hydrogen Production with CO_2 Capture[J]. *International Journal of Hydrogen Energy*, 2016, 41: 4969-4992.

[2] Dong L, Miao G Y, Wen W G. China's Carbon Neutrality Policy: Objectives, Impacts and Paths[J]. *East Asian Policy*, 2021, 13(1): 5-18.

[3] Melaina M W, Antonia O, Penev M. Blending Hydrogen into Natural Gas Pipeline Networks: A Review of Key Issues [M]. *Golden*: *National Renewable Energy Lab*, 2013.

[4] Chterev I, Boxx I. Effect of Hydrogen Enrichment on the Dynamics of a Lean Technically Premixed Elevated Pressure Flame[J]. *Combustion and Flame*, 2021, 225: 149-159.

[5] Jigjid K, Tamaoki C, Minamoto Y, et al. Data Driven

Analysis and Prediction of MILD Combustion Mode[J]. *Combustion and Flame*, 2021, 223: 474-485.

[6] Roy R, Gupta A K. Flame Structure and Emission Signature in Distributed Combustion[J]. *Fuel*, 2020, 262: 1-13.

[7] Öztuna S, Büyükakın M K. Effects of Hydrogen Enrichment of Methane on Diffusion Flame Structure and Emissions in a Back-Pressure Combustion Chamber[J]. *International Journal of Hydrogen Energy*, 2020, 45: 5971-5986.

[8] Lingstädt T, Grimm F, Krummrein T, et al. Atmospheric Experimental Investigations of a Jet-Stabilized SOFC Off-Gas Combustor for a Hybrid Power Plant Operated with Biogas[C]. *San Diego*: *AIAA Scitech* 2019 *Forum*, 2019.

[9] Zornek T, Mosbach T, Aigner M. Optical Measurements of a Lower Calorific Values-Combustor Operated in a Micro Gas Turbine with Various Fuel Compositions[J]. *Journal of Engineering for Gas Turbines and Power*, 2018, 141: 041032.

[10] Huang M M, Shao W W, Xiong Y, et al. Effect of Fuel Injection Velocity on MILD Combustion of Syngas in Axially-Staged Combustor[J]. *Applied Thermal Engineering*, 2014, 66: 485-492.

[11] Mardani A, Mahalegi H K M. Hydrogen Enrichment of Methane and Syngas for MILD Combustion[J]. *International Journal of Hydrogen Energy*, 2019, 44: 9423-9437.

[12] Sadanandan R, Lückerath R, Meier W, et al. Flame Characteristics and Emissions in Flameless Combustion under Gas Turbine Relevant Conditions[J]. *Journal of Propulsion and Power*, 2011, 27: 970-980.

[13] Zhang H, Zhang Z, Xiong Y, et al. Experimental and Numerical Investigations of MILD Combustion in a Model Combustor Applied for Gas Turbine[C]. *Oslo*: *ASME Turbo Expo* 2018: *Turbomachinery Technical Conference and Exposition. American Society of Mechanical Engineers Digital Collection*, 2018.

[14] Karyeyen S, Feser J S, Gupta A K. Hydrogen Concentration Effects on Swirl-Stabilized Oxy-Colorless Distributed Combustion[J]. *Fuel*, 2019, 253: 772-780.

[15] Liu X, Shao W W, Tian Y, et al. Investigation of H_2/CH_4-Air Flame Characteristics of a Micromix Model Burner at Atmosphere Pressure Condition[C]. *Oslo*: *ASME Turbo Expo* 2018: *Turbomachinery Technical Conference and Exposition. American Society of Mechanical Engineers Digital Collection*, 2018.

[16] Deng X, Xiong Y, Yin H, et al. Numerical Study of the Effect of Nozzle Configurations on Characteristics of MILD Combustion for Gas Turbine Application[J]. *Journal of Energy Resources Technology*, 2016, 138(4): 1-8.

[17] Cavaliere A, De Joannon M. Mild Combustion[J]. *Progress in Energy and Combustion Science*, 2004, 30(4): 329-366.

[18] Parente A, Galletti C, Tognotti L. Effect of the Combustion Model and Kinetic Mechanism on the MILD Combustion in an Industrial Combustor Fed with Hydrogen Enriched Fuels[J]. *International Journal of Hydrogen Energy*, 2008, 33(24): 7553-7564.

[19] Lingstädt T, Drude A M, Grimm F, et al. Numerical Investigation of a Jet-Stabilized Combustion System Operated with Low-Calorific SOFC Off-Gas[C]. *San Diego*: *AIAA Scitech* 2019 *Forum*, 2019.

[20] Frassoldati A, Sharma P, Cuoci A, et al. Kinetic and Fluid Dynamics Modeling of Methane/Hydrogen Jet Flames in Diluted Coflow[J]. *Applied Thermal Engineering*, 2010, 30(4): 376-383.

[21] Lewandowski M T, Ertesvåg I S. Analysis of the Eddy Dissipation Concept Formulation for MILD Combustion Modelling[J]. *Fuel*, 2018, 224: 687-700.

[22] Li Z S, Li B, Sun Z W, et al. Turbulence and Combustion Interaction: High Resolution Local Flame Front Structure Visualization Using Simultaneous Single-Shot PLIF Imaging of CH, OH, and CH_2O in a Piloted Premixed Jet Flame[J]. *Combustion and Flame*, 2010, 157(6): 1087-1096.

(编辑：刘萝威)